

# Preparation of Poly (ethylene oxide)-graft-poly (acrylic acid) Copolymer Stabilized Iron Oxide Nanoparticles Via an *In Situ* Templated Process

Pengpeng Li, Junlian Huang

The Key Laboratory of Molecular Engineering of Polymer, State Education Ministry of China, Department of Macromolecular Science, Fudan University, Shanghai 200433, China

Received 30 August 2007; accepted 20 November 2007

DOI 10.1002/app.27801

Published online 28 March 2008 in Wiley InterScience (www.interscience.wiley.com).

**ABSTRACT:** Superparamagnetic iron oxide nanoparticles were prepared in the presence of poly (ethylene oxide)-graft-poly (acrylic acid) copolymers via an *in situ* templated coprecipitation process. The resulted composite nanoparticles consisted of clusters of iron oxide monocrystals embedded inside the polymer chains, and were highly dispersible in aqueous solution. In these graft copolymers, the PAA segments were chemisorbed onto the Fe<sub>3</sub>O<sub>4</sub> nanoparticle surface through their carboxylic acid groups by forming carboxylate groups with the Fe atoms, while PEO segments as the stabilizers extended into the water matrix.

Thus the composite nanoparticles exhibited narrow size distribution by the dynamic light scattering measurement. X-ray diffraction and magnetometer data confirmed the crystalline structure and superparamagnetic property of the particles. This procedure provided a good choice for preparing stable iron oxide magnetic nanoparticles with PEO modified surfaces. © 2008 Wiley Periodicals, Inc. *J Appl Polym Sci* 109: 501–507, 2008

**Key words:** graft copolymer; nanocomposites; templet; poly (ethylene oxide); poly (acrylic acid); iron oxide

## INTRODUCTION

Recently, the interest in preparation of magnetic nanoparticles and investigation of their biomedical application is growing.<sup>1–5</sup> Several types of iron oxides have been investigated in the field of nano-sized magnetic particles. Among them the magnetite Fe<sub>3</sub>O<sub>4</sub> is a very promising candidate since its biocompatibility has already been proven.<sup>1</sup>

There have been various methods developed for the preparation of magnetic nanoparticles.<sup>6</sup> The most commonly used protocol involves coprecipitation of ferrous and ferric ions in basic solutions.<sup>7–12</sup> However, the nanoparticles during the process of coprecipitation are likely to aggregate. Consequently, how to prevent aggregation between the nanoparticles during synthesis of Fe<sub>3</sub>O<sub>4</sub> has received considerable attention because the actual applications need well-dispersed magnetic nanoparticles. Recently, polymers such as dextran, polyvinyl alcohol (PVA), and diethylaminoethyl-starch were added to coat the particles for better stability before or after the formation of iron oxide particles.<sup>13</sup> However, the loose associa-

tion of polymers may fall off after injected into the body. An improved approach is to initiate the iron oxide coprecipitation process in polymer solutions such as carboxylated dendrimer<sup>14</sup> or poly (acrylic acid).<sup>10</sup> In these cases the polymers were thought to provide templates for mineral nucleation and to regulate particle growth.

Poly (ethylene oxide) (PEO) is a widely investigated polymer, which is used to form covalent bonds with biological macromolecules and modify the surfaces for many pharmaceutical and biotechnical applications.<sup>15,16</sup> The nanoparticle surfaces modified with PEO showed extended life in the circulation of the blood stream,<sup>1</sup> nonimmunogenic, nonantigenic and protein resistant.<sup>17,18</sup>

Immobilization of PEO macromolecules on iron oxide for biocompatibility has been achieved via a variety of approaches, which include self-assembly of bifunctional trifluoroethyl ester PEO silane on metal oxide based nanoparticles,<sup>19</sup> surface-initiated atom transfer radical polymerization of poly(ethylene oxide) monomethacrylate,<sup>17</sup> and thermal decomposition of ferric triacetylacetonate (Fe(acac)<sub>3</sub>) in 2-pyrrolidone in the presence of MPEO-COOH.<sup>20</sup> Stable aqueous iron oxide nanoparticle dispersions were also prepared by coprecipitation of ferrous and ferric aqueous solution in the presence of a base and the graft copolymer poly (glycerol monoacrylate)-g-poly (PEO methyl ether acrylate) (PGA-g-PEO).<sup>11</sup> As it is well known that the poly (acrylic acid) (PAA)

Correspondence to: Junlian Huang (jlhuang@fudan.edu.cn).

Contract grant sponsor: National Natural Science Foundation of China; contract grant number: 20574010.

**TABLE I**  
Synthesized Stars and Linear Graft Copolymers Poly (ethylene oxide)-graft-poly (acrylic acid)

Sample <sup>a</sup>	Structure <sup>b</sup>	$R_T$ <sup>c</sup>	$N_{PEO}$ <sup>d</sup>	$N_{PAA}$ <sup>d</sup>	$M_n$ <sup>e</sup>	$M_w/M_n$ <sup>f</sup>	(PAA/PEO) <sup>g</sup>
S1	A	3/1	176	440	43,736	1.21	2.50
S2	A	12/1	208	240	28,000	1.19	1.15
L	B	9.5/1	124	208	22,256	1.15	1.68

<sup>a</sup> S1, [poly(EO<sub>3-co</sub>-Gly)<sub>11-g</sub>-PAA<sub>10</sub>]<sub>4</sub>; S2, [poly(EO<sub>12-co</sub>-Gly)<sub>4-g</sub>-PAA<sub>15</sub>]<sub>4</sub>; L, poly(EO<sub>9.5-co</sub>-Gly)<sub>13-g</sub>-PAA<sub>16</sub>.

<sup>b</sup> A, star graft copolymer; B, linear graft copolymer.

<sup>c</sup> The molar ratio of EO to Gly in the backbone of graft copolymer.

<sup>d</sup>  $N_{PEO}$  and  $N_{PAA}$  means the number of PEO and PAA segment in the copolymer, respectively.

<sup>e</sup> Number average molecular weight ( $M_n$ ) calculated from <sup>1</sup>H NMR.

<sup>f</sup> Molecular weight distribution ( $M_w/M_n$ ) obtained before hydrolysis of the *t*BA ester groups which were determined by GPC.

<sup>g</sup> The molar ratio of PAA and PEO segments in the copolymers.

can provide templates *in situ* in preparation of iron oxide nanoparticles and PEO modification of iron oxide nanoparticles surfaces can ensure its potential usage *in vivo*, therefore a method was developed to prepare poly (ethylene oxide)-graft-poly (acrylic acid) copolymer and poly (ethylene oxide)-graft-poly (acrylic acid) copolymer with four arms which were employed to stabilize iron oxide nanoparticles via an *in situ* templated process.

## EXPERIMENTAL

### Materials

Fe(II) chloride tetrahydrate (99%), Fe(III) chloride hexahydrate(97%) were purchased from Fluka and used as supplied. Other chemicals (Sinopharm Chemical Reagent) were of analytical grade and used without further purification. Distilled and deionized water was used throughout the work.

### Synthesis of star graft copolymers poly (ethylene oxide)-graft-poly (acrylic acid)<sup>21</sup>

Briefly, the general route to synthesize the star graft copolymer was (i) Synthesis of [poly (EO-*co*-EEGE)]<sub>4</sub> by anionic ring-opening copolymerization of ethylene oxide (EO) and ethoxyethyl glycidyl ether (EEGE), using pentaerythritol as the precursor, mixture of dimethyl sulfoxide and tetrahydrofuran as the solvent, and diphenylmethyl potassium (DPMK) as the deprotonating agent. (ii) Removal of the ethoxyethyl groups of EEGE units of the copolymers by hydrolysis to obtain hydroxyl groups, and then the reaction of pending hydroxyl groups with 2-bromoisobutyryl bromide to form the macroinitiator. (iii) Copper-mediated atom transfer radical polymerization (ATRP) of *tert*-butyl acrylate (*t*BA) in acetone at 60°C using macroinitiator. (iv) Hydrolysis of the *t*BA ester groups to obtain the free acid form of copolymers using an excess of trifluoroacetic acid in

CH<sub>2</sub>Cl<sub>2</sub>. The copolymer with linear graft structure was obtained similarly. (The characterization of these copolymers was listed in Table I.)

### Preparation of iron oxide/polymer composite nanoparticles

In a typical process (sample SF2 in Table II), 0.1247 g of graft copolymer, 0.2910 g of FeCl<sub>3</sub> · 6H<sub>2</sub>O and 0.1102 g of FeCl<sub>2</sub> · 4H<sub>2</sub>O were dissolved in 50 mL of water with vigorous stirring at room temperature under N<sub>2</sub>. To initiate iron oxide formation, NaOH aqueous solution (1 mol/L) was used to basify the solution by drop-wise addition until the color of the mixture turned from orange to black. The reaction was carried out under N<sub>2</sub> with stirring at 400 rpm for 30 min. Afterwards the solution was heated to 80°C for 60 min for crystalline maturation. Composite magnetic nanoparticles were purified and harvested by ultracentrifugation at 10,000 rpm for 5 min followed by lyophilization.

**TABLE II**  
DLS Measurement of Pure Fe<sub>3</sub>O<sub>4</sub> Nanoparticles, and Composite Fe<sub>3</sub>O<sub>4</sub> Nanoparticles Prepared with Different Amount of Polymer

Sample	Polymer used <sup>a</sup>	$R_T$ <sup>b</sup>	$D_h$ <sup>c</sup> nm	PI <sup>c</sup>	TGA <sup>d</sup>	TEM <sup>e</sup> nm
SF1	None	–	574	–	98%	–
SF2	S1	1/1	164	0.345	69%	10
SF3	S1	1/2	165	0.152	87%	–
SF4	S1	1/3	198	0.091	90%	20
SF5	S2	1/1	105	0.148	73%	10
SF6	L	1/1	215	0.300	65%	15

<sup>a</sup> Polymer used: S1, S2, and L have the same meaning as Table I.

<sup>b</sup> The mass ratio of polymer used to Fe<sub>3</sub>O<sub>4</sub>.

<sup>c</sup> The hydrodynamic diameter ( $D_h$ ) and size distribution of nanoparticles (PI) measured by DLS.

<sup>d</sup> Result of TGA measurement.

<sup>e</sup> Diameter of Fe<sub>3</sub>O<sub>4</sub> nanoparticles obtained from TEM.

Samples of blank iron oxide particles were prepared parallel under the same condition but without the polymer as templates.

### Observation of Fe<sub>3</sub>O<sub>4</sub> nanoparticles by transmission electron microscope

A drop of the diluted solutions of the preparations was deposited on carbon films supported by copper grids and air-dried at room temperature. Transmission electron microscope (TEM) morphology study was performed on a Hitachi H-600 electron microscope operated at an accelerating voltage of 75 kV.

### Particle size analysis

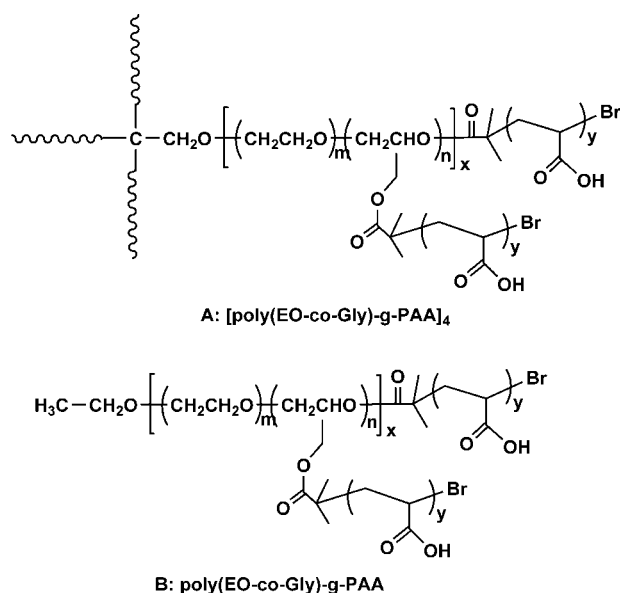
The particle size distribution of the composite magnetic nanoparticles was determined by dynamic light scattering measurement using a commercial laser light scattering (LLS) spectrometer (Malvern Autosizer 4700). The average hydrodynamic diameter and polydispersity index was evaluated.

### FTIR characterization

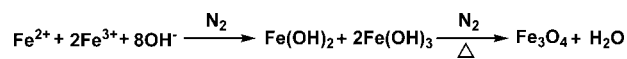
The lyophilized magnetic nanoparticles were grounded with KBr for FTIR measurement by Magna-550 Fourier transform infrared spectrometer.

### TGA and XRD analysis

The freeze-dried composite magnetic nanoparticles were subjected to TGA analysis (Perkin-Elmer Pyris 1). The temperature was raised from 50 to 800°C at a heating rate of 15°C/min under N<sub>2</sub>. Additionally, X-ray diffraction (XRD) measurements were taken to investigate the crystal structure of the particles using X'Pert PRO X-ray powder diffractometer with CuKα



**Scheme 1** Structures of star and linear graft copolymers.



**Scheme 2** Chemical equations to obtain Fe<sub>3</sub>O<sub>4</sub> by the chemical coprecipitation.

(1.541 Å) radiation (40 kV, 40 mA), and the samples were exposed at a scan rate of  $2\theta = 0.0007 \text{ s}^{-1}$  in the range of 20° and 90°.

### Measurement of magnetization of composite Fe<sub>3</sub>O<sub>4</sub> nanoparticles<sup>13</sup>

Magnetic characterization of the nanoparticles was carried out on EG and G Princeton Applied Research Model 155 vibrating sample magnetometer at room temperature with maximum applied field of 3 T.

## RESULTS AND DISCUSSION

The general structures of the star graft copolymers with four-arms (A) and linear graft copolymers (B) are shown in Scheme 1, and the data pertaining to the composition of the different samples are given in Table I. Details of the copolymer synthesis and their characterization other than those given in Table I were reported elsewhere.<sup>21</sup>

### Preparation and characterization of iron oxide/polymer composite nanoparticles

The traditional method for preparation of Fe<sub>3</sub>O<sub>4</sub> nanoparticles was the chemical coprecipitation of ferric and ferrous salts in alkaline medium as shown in Scheme 2.

However, the Fe<sub>3</sub>O<sub>4</sub> nanoparticles synthesized by this traditional method would aggregate easily as Figure 1(A) showed.

To prevent aggregation, the graft copolymers poly(ethylene oxide)-graft-poly(acrylic acid) [poly(EO<sub>12</sub>-co-Gly)<sub>4</sub>-g-PAA<sub>15</sub>]<sub>4</sub> were used for modification of the traditional chemical coprecipitation method. The obtained Fe<sub>3</sub>O<sub>4</sub>/polymer composite nanoparticles could be suspended homogeneously and stably in

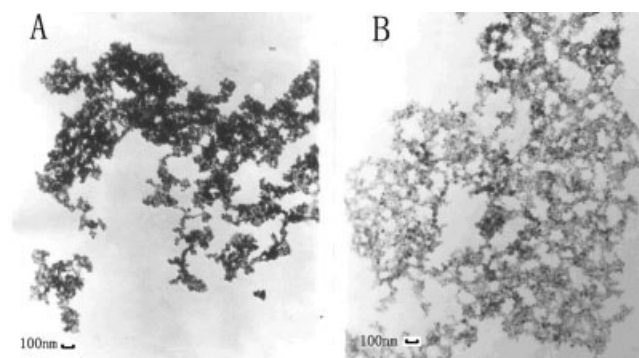
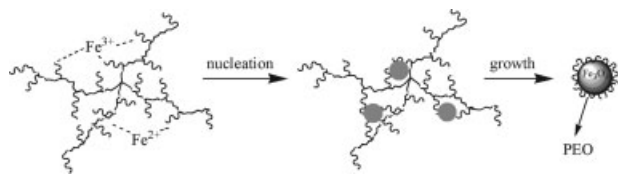


**Figure 1** TEM images of iron oxide nanoparticles: (A) without polymer; (B) in the presence of polymer.



**Scheme 3** Strategy adopted for the synthesis of iron oxide nanoparticles in the presence of polymer.

water as shown in Figure 1(B) (SF5 in Table II). The proposed mechanism was shown in Scheme 3.

At first the  $\text{Fe}^{2+}$  and  $\text{Fe}^{3+}$  ions were coordinated with carboxylic acid groups of PAA segments to form the complexes, and then the nucleation of  $\text{Fe}_3\text{O}_4$  particles was promoted by carboxylic acid groups on the PAA segments in the presence of the NaOH aqueous solution. In this case the PAA segments were acted as the template for  $\text{Fe}_3\text{O}_4$  nucleation, but the growth of particles would be hindered by the PEO segments, so the size of the particles was only about 10–20 nm (observed by TEM), which was smaller than the traditional product.

From the chemical equation of  $\text{Fe}_3\text{O}_4$  precipitation, the suitable mole concentration ratio of Fe (II) to Fe (III) should be 1/2 for the synthesis of  $\text{Fe}_3\text{O}_4$  nanoparticles, and the pH should be higher than 6.93. In our system, the mole ratio of Fe (II) to Fe (III) was 1/2 and the pH values of ferrofluid after synthesis were between 9 and 10. Therefore, these conditions of reaction were suitable to form  $\text{Fe}_3\text{O}_4$  nanoparticles.

The functional groups of the obtained iron oxide nanoparticles can be measured by FTIR. Figure 2 shows a comparison between the FTIR spectra of the pure graft copolymer [poly( $\text{EO}_3\text{-co-Gly}$ )<sub>11-g-PAA</sub>]<sub>4</sub>, pure  $\text{Fe}_3\text{O}_4$  nanoparticles, and composite  $\text{Fe}_3\text{O}_4$  nanoparticles with different amount of copolymer [poly( $\text{EO}_3\text{-co-Gly}$ )<sub>11-g-PAA</sub>]<sub>4</sub>. It was reported that the characteristic absorption bands of the Fe—O bond of bulk  $\text{Fe}_3\text{O}_4$  were at  $570\text{ cm}^{-1}$ .<sup>22</sup> However, when the size of  $\text{Fe}_3\text{O}_4$  particles was reduced to

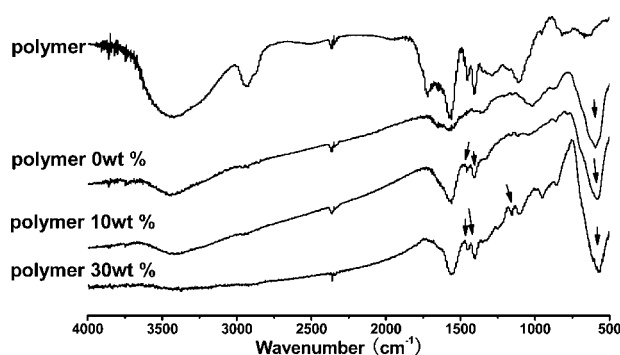


**Figure 2** FTIR analysis of polymer, pure  $\text{Fe}_3\text{O}_4$  nanoparticles, and composite  $\text{Fe}_3\text{O}_4$  nanoparticles with different amount of polymer [poly( $\text{EO}_3\text{-co-Gly}$ )<sub>11-g-PAA</sub>]<sub>4</sub>.

nanoscale dimensions, the surface bond force constant was increased due to the effect of finite size of nanoparticles, in which the breaking of a large number of bonds for surface atoms resulted in the rearrangement of nonlocalized electrons on the particle surface.<sup>23</sup> Therefore, the FTIR spectrum of  $\text{Fe}_3\text{O}_4$  nanoparticles would exhibit a blue shift and the characteristic absorption bands of the Fe—O bond were shifted to high wave numbers of about  $580\text{ cm}^{-1}$ , as shown in Figure 2.

The characteristic absorption band of pure  $\text{Fe}_3\text{O}_4$  nanoparticles at  $580\text{ cm}^{-1}$  also appeared in the spectrum of the composite  $\text{Fe}_3\text{O}_4$  nanoparticles. In addition, the FTIR spectrum of the composite  $\text{Fe}_3\text{O}_4$  nanoparticles shows that the peak at  $1710\text{ cm}^{-1}$  for carbonyl of PAA segments was shrank and two new peaks at  $1452$  and  $1405\text{ cm}^{-1}$  appeared due to the binding of the carboxylic acid groups to the surface of the nanoparticles to form carboxylate groups,<sup>24</sup> these new peaks corresponded to the  $\text{COO}^-$  anti-symmetric vibration and the  $\text{COO}^-$  symmetric vibration indicated the bidentate bonding of the carbonyl groups to the surface Fe atoms.<sup>25,26</sup> The remaining but shrunken peak at  $1710\text{ cm}^{-1}$  for C=O stretch indicated some fraction of the PAA segments were bonded to nanoparticles either in monodentate form or as an acid.<sup>25,26</sup> It can also be observed that when the amount of polymer in the composite  $\text{Fe}_3\text{O}_4$  nanoparticles was increased to 30 wt %, the bonds of aliphatic acid at  $1105\text{--}1159\text{ cm}^{-1}$  appeared. Consequently, the interaction between PAA segments and  $\text{Fe}_3\text{O}_4$  nanoparticles was through chemical bonding as shown in Scheme 3.

To investigate the effect of copolymer on the properties of  $\text{Fe}_3\text{O}_4$  nanoparticles, the synthesized composite  $\text{Fe}_3\text{O}_4$  nanoparticles were analyzed by XRD and the result was shown in Figure 3.

It is well known that the characteristic peaks of standard  $\text{Fe}_3\text{O}_4$  crystal (isometric-hexoctahedral

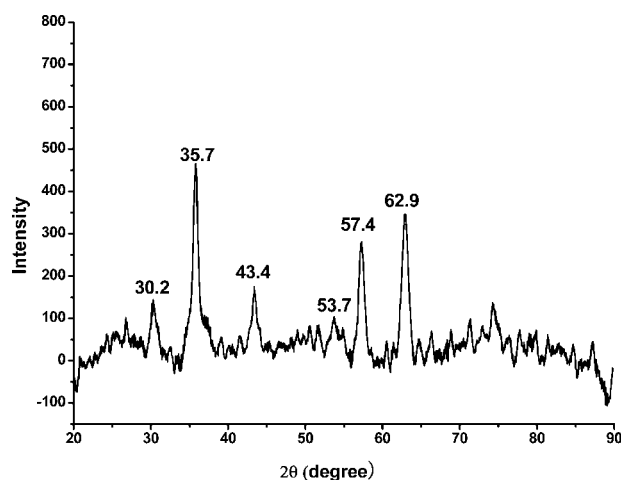


**Figure 3** XRD pattern of composite  $\text{Fe}_3\text{O}_4$  nanoparticles prepared in the presence of graft copolymer (SF2 in Table II).

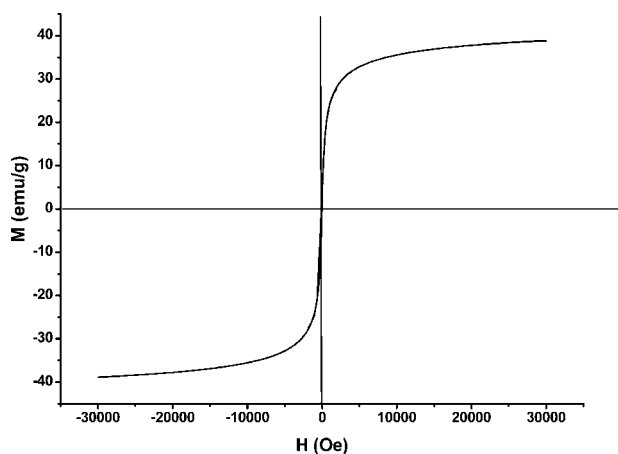


**Figure 4** Magnetization curve of magnetic composite nanoparticles (SF2 in Table II).

crystal system) had six diffraction peaks at  $2\theta = 30.2^\circ, 35.7^\circ, 43.4^\circ, 53.7^\circ, 57.4^\circ, 62.9^\circ$ .<sup>10</sup> The positions and relative intensities of XRD peaks of the obtained composite  $\text{Fe}_3\text{O}_4$  nanoparticles shown in Figure 3 were consistent with the standard pattern, except for the broadening of the peaks.<sup>13</sup> The broadening of the peaks was probably due to the matrix constrain of the nanosized particles.

The magnetization curve of the nanoparticles confirmed that the composite nanoparticles indeed have superparamagnetic properties (Fig. 4). The saturation magnetization was about 38 emu/g, and the coercive force was 0 Oersteds. These data were comparable to what had been reported in the literature for iron oxide nanoparticles synthesized using other polymer.<sup>9,10</sup> Outwardly, the value of saturation magnetization was lower than that of the pure  $\text{Fe}_3\text{O}_4$  nanoparticles (26 nm, 50 emu/g),<sup>9</sup> but the mass of copolymers in the composite nanoparticles (67% in weight) did not make contribution to the saturation magnetization, the calculated value is about 56 emu/g after subtracting the mass of copolymers. This result proved that the polymer template did not influence the magnetization properties of  $\text{Fe}_3\text{O}_4$  nanoparticles.

Figure 5 shows the TGA analysis of pure  $\text{Fe}_3\text{O}_4$  nanoparticles and composite  $\text{Fe}_3\text{O}_4$  nanoparticles prepared with different amount of polymer. As Figure 5 indicated that the pure  $\text{Fe}_3\text{O}_4$  nanoparticles showed insignificant weight loss from 100 to 800°C. However, during degradation of the composite  $\text{Fe}_3\text{O}_4$  nanoparticles prepared with graft copolymer. There were three stages in the TGA curve: in the first-stage, the weight loss occurred below 200°C, it may attribute to the small quantity of the water in the sample; in the second stage, the decomposition between the temperature 200–400°C can be attributed to the loss of PEO chains; the loss above 400°C in the third stage was due to decomposition of PAA

segments. The interesting decomposition at 700°C may be due to the deoxidization of a little  $\text{Fe}_2\text{O}_3$  particles<sup>10</sup> to form  $\text{Fe}_3\text{O}_4$  at 700°C under  $\text{N}_2$  atmosphere. Therefore, both the decomposition of PEO, PAA and the deoxidization of  $\text{Fe}_2\text{O}_3$  were the main causes for the weight loss of magnetic composite nanoparticles in the TGA analysis. In Figure 5, it was observed that the TGA curves of SF4 and SF6 were different. It may attribute to the lower copolymer content of SF4 than SF6, therefore the third stage in the curve was subtle.

The residual weight percentage of magnetic composite nanoparticles in the TGA analysis was the contribution of the  $\text{Fe}_3\text{O}_4$  nanoparticles. The results indicate that the weight ratio of graft copolymers to  $\text{Fe}_3\text{O}_4$  nanoparticles was nearly 1/2 (in the case of SF6). Theoretically, from the feed composition the weight ratio of graft copolymers to  $\text{Fe}_3\text{O}_4$  nanoparticles in the composite  $\text{Fe}_3\text{O}_4$  nanoparticles was about 1/1. The difference may be attributed to the property that some polymers were physically adsorbed to the surface of  $\text{Fe}_3\text{O}_4$  nanoparticles and the force of adsorption was weak. During the ultra-centrifugation before the TGA measurement these polymers fell off from the surface of  $\text{Fe}_3\text{O}_4$  nanoparticles.

#### The size distribution and morphology of iron oxide/polymer composite nanoparticles

Four arm star graft copolymers ([poly( $\text{EO}_{3-co}\text{-Gly}$ )<sub>11</sub>-g-PAA<sub>10</sub>]<sub>4</sub> and [poly( $\text{EO}_{12-co}\text{-Gly}$ )<sub>4</sub>-g-PAA<sub>15</sub>]<sub>4</sub>) with different grafting densities were used to stabilize iron oxide nanoparticles. Linear graft copolymer poly( $\text{EO}_{9.5-co}\text{-Gly}$ )<sub>13</sub>-g-PAA<sub>16</sub> was also used for comparison. The results were listed in Table II.

As Table II showed, the composite  $\text{Fe}_3\text{O}_4$  nanoparticles have smaller hydrodynamic diameter than

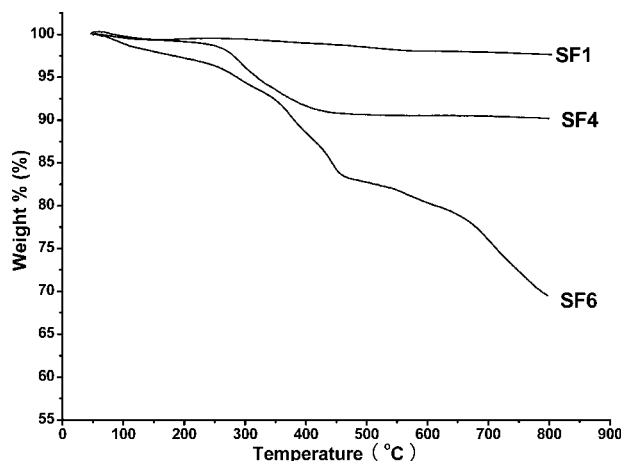


**Figure 5** TGA analysis of the pure  $\text{Fe}_3\text{O}_4$  nanoparticles, and composite  $\text{Fe}_3\text{O}_4$  nanoparticles prepared with different amount of polymer.

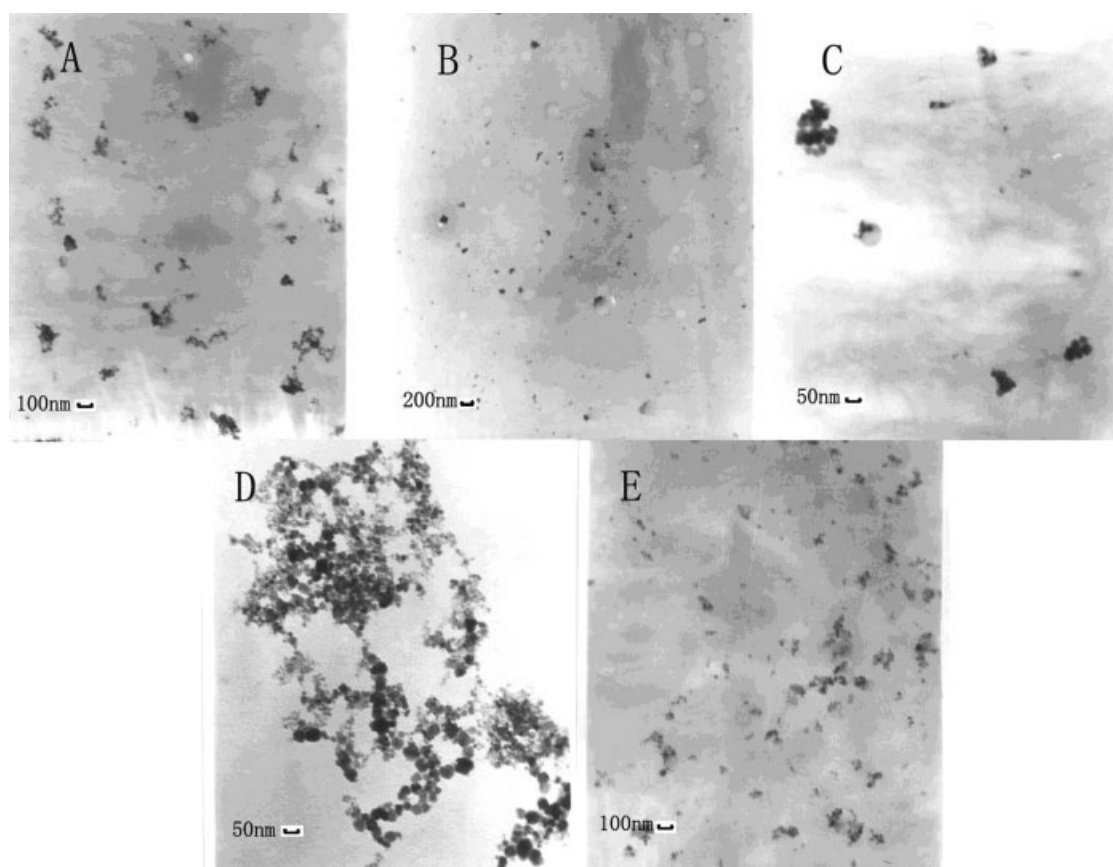


**Figure 6** TEM images of iron oxide nanoparticles prepared with polymer: (A) SF2, (B) and (C) SF4, (D) SF5, (E) SF6.

pure  $\text{Fe}_3\text{O}_4$  nanoparticles whatever kinds or amount of polymer used. The narrow size distributions of composite  $\text{Fe}_3\text{O}_4$  nanoparticles demonstrated that they have almost the same size. The mass ratio of polymer used to  $\text{Fe}_3\text{O}_4$  may also have influence on the size and size distribution of composite  $\text{Fe}_3\text{O}_4$  nanoparticles. For example, when the same copolymer [poly( $\text{EO}_3$ -*co*-Gly) $_{11}$ -*g*-PAA $_{10}$ ] $_4$  was used in the process of preparation, if the mass ratio of polymer used to  $\text{Fe}_3\text{O}_4$  was changed from 1/1 to 1/3, the diameters of composite  $\text{Fe}_3\text{O}_4$  nanoparticles would be increased from 164 nm to 198 nm, but the particle size distribution becomes narrower. When the same mass ratio of polymer to  $\text{Fe}_3\text{O}_4$  was used, composite  $\text{Fe}_3\text{O}_4$  nanoparticles prepared in the presence of polymer [poly( $\text{EO}_{12}$ -*co*-Gly) $_4$ -*g*-PAA $_{15}$ ] $_4$  have smaller diameter and narrower size distribution than that prepared in the presence of polymer [poly( $\text{EO}_3$ -*co*-Gly) $_{11}$ -*g*-PAA $_{10}$ ] $_4$ . It may be attributed to the different ratio of PAA/PEO segments in the used graft copolymer. As it can be seen in Table I, the ratio of PAA/PEO in [poly( $\text{EO}_3$ -*co*-Gly) $_{11}$ -*g*-PAA $_{10}$ ] $_4$  is 2.50 and the value in [poly( $\text{EO}_{12}$ -*co*-Gly) $_4$ -*g*-PAA $_{15}$ ] $_4$  is 1.15, so the larger proportion of PEO segments may prove to be a better template in the preparation

process. Linear graft copolymer poly( $\text{EO}_{9.5}$ -*co*-Gly) $_{13}$ -*g*-PAA $_{16}$  was also used to prepare the composite  $\text{Fe}_3\text{O}_4$  nanoparticles; the diameter of the nanoparticles was larger than that prepared in the presence of four-arm star copolymer. This result demonstrates that the star graft copolymer has advantage over the linear graft copolymer in restraining the growth of nanoparticles because of their more confined structures.

The resulted composite particles were examined under TEM and were seen as clusters of a few small iron oxide dots (Fig. 6). Each individual dot was about 10–20 nm in diameter, and they clustered together to form dispersed particles. The diameter values determined by TEM were smaller than the hydrodynamic diameter measured by DLS. It may be attributed to the fact that the associated polymer chains could be measured by DLS, but they were not visible under TEM. Nevertheless, these composite particles can be still estimated by the general morphology and arrangement of iron oxide cluster using TEM. Therefore, although some monocrystalline spheres were closely packed together, they were still distinctively separated with clear boundaries.

## CONCLUSIONS

Iron oxide/polymer composite nanoparticles were prepared using a coprecipitation method in the presence of poly (ethylene oxide)-graft-poly (acrylic acid) copolymer via an *in situ* templated process. The star graft copolymers with larger proportion of PEO segments provided the better template in the preparation process. The obtained composite nanoparticles with superparamagnetic properties are water-soluble and well-dispersed. This kind of iron oxide/polymer composite nanoparticle with PEO modified surface may find the potential application in biomedical fields.

## References

1. Gupta, A. K.; Gupta, M. *Biomaterials* 2005, 26, 3995.
2. Hilger, I.; Trost, R.; Reichenbach, J. R.; Linss, W.; Lisy, M. R.; Berndt, A.; Kaiser, W. A. *Nanotechnology* 2007, 18, 1.
3. McCarthy, J. R.; Kelly, K. A.; Sun, E. Y.; Weissleder, R. *Nanomedicine* 2007, 2, 153.
4. Mornet, S.; Vasseur, S.; Grasset, F.; Duguet, E. *J Mater Chem* 2004, 14, 2161.
5. Taboada, E.; Rodriguez, E.; Roig, A.; Oro, J.; Roch, A.; Muller, R. N. *Langmuir* 2007, 23, 4583.
6. Cushing, B. L.; Kolesnichenko, V. L.; O'Connor, C. J. *Chem Rev* 2004, 104, 3893.
7. Badescu, R.; Condurache, D.; Ivanoiu, M. *J Magn Magn Mater* 1999, 202, 197.
8. Harris, L. A.; Goff, J. D.; Carmichael, A. Y.; Riffle, J. S.; Harburn, J. J.; St Pierre, T. G.; Saunders, M. *Chem Mater* 2003, 15, 1367.
9. Lee, J.; Isobe, T.; Senna, M. *J Colloid Interface Sci* 1996, 177, 490.
10. Lin, C. L.; Lee, C. F.; Chiu, W. Y. *J Colloid Interface Sci* 2005, 291, 411.
11. Wan, S. R.; Huang, J. S.; Yan, H. S.; Liu, K. L. *J Mater Chem* 2006, 16, 298.
12. Wan, S. R.; Zheng, Y.; Liu, Y. Q.; Yan, H. S.; Liu, K. L. *J Mater Chem* 2005, 15, 3424.
13. Liu, S. P.; Wei, X. H.; Chu, M. Q.; Peng, J. L.; Xu, Y. H. *Colloid Surf B-Biointerfaces* 2006, 51, 101.
14. Strable, E.; Bulte, J. W. M.; Moskowitz, B.; Vivekanandan, K.; Allen, M.; Douglas, T. *Chem Mater* 2001, 13, 2201.
15. Roberts, M. J.; Bentley, M. D.; Harris, J. M. *Adv Drug Deliv Rev* 2002, 54, 459.
16. Veronese, F. M. *Biomaterials* 2001, 22, 405.
17. Hu, F. X.; Neoh, K. G.; Cen, L.; Kang, E. T. *Biomacromolecules* 2006, 7, 809.
18. Zhang, M. Q.; Desai, T.; Ferrari, M. *Biomaterials* 1998, 19, 953.
19. Kohler, N.; Sun, C.; Fichtenholtz, A.; Gunn, J.; Fang, C.; Zhang, M. Q. *Small* 2006, 2, 785.
20. Li, Z.; Wei, L.; Gao, M. Y.; Lei, H. *Adv Mater* 2005, 17, 1001.
21. Li, P. P.; Li, Z. Y.; Huang, J. L. *Macromolecules* 2007, 40, 491.
22. Waldron, R. D. *Phys Rev* 1995, 99, 1727.
23. Ma, M.; Zhang, Y.; Yu, W.; Shen, H. Y.; Zhang, H. Q.; Gu, N.; *Colloid Surf A-Physicochem Eng Asp* 2003, 212, 219.
24. Moore, R. G. C.; Evans, S. D.; Shen, T.; Hodson, C. E. C. *Physica E* 2001, 9, 253.
25. Liu, Q. X.; Xu, Z. H. *Langmuir* 1995, 11, 4617.
26. Shukla, N.; Liu, C.; Jones, P. M.; Weller, D. *J Magn Magn Mater* 2003, 266, 178.